АТОМНА ЕНЕРГЕТИКА
ATOMIC ENERGY

УДК 621.039.76 https://doi.org/10.15407/jnpae2025.04.320

O. V. Mykhailov*, M. V. Saveliev, A. O. Doroshenko

Institute for Safety Problems of Nuclear Power Plants, National Academy of Sciences of Ukraine, Chornobyl, Kyiv region, Ukraine

*Corresponding author: o.mikhailov@ispnpp.kiev.ua

ANALYSIS OF LONG-TERM MONITORING DATA AROUND THE AREA OF LOCALIZATION OF NUCLEAR-HAZARDOUS CLUSTERS IN THE "SHELTER" OBJECT

The results of a comprehensive analysis of neutron flux density (NFD), gamma-radiation exposure dose rate (GDR), dynamics of concrete temperature and air humidity in the vicinity of nuclearly hazardous fuel-containing material cluster (NHC) in room 305/2 of the Chornobyl "Shelter" Object, are demonstrated. In line with the data obtained from the Nuclear Safety Monitoring System between 2017 and 2024, typical trends in the dynamics of NFD and GDR are established. Seasonal fluctuations in air humidity and concrete temperature collected by meteorological equipment and Expert Research System were also examined, and their partial influence on NFD dynamics at different monitoring points was highlighted. The correlation between measured parameters from weak to strong was identified, depending on the sensor location relative to the NHC area localization. A new insight into the spatial and temporal behaviour of radiation and thermal fields around NHC was obtained, which highlights the importance of continuous monitoring to ensure nuclear safety of the "Shelter" Object and demands that the research in this area should be continued.

Keywords: Chornobyl NPP, "Shelter" Object, nuclearly hazardous clusters, neutron flux density, gamma-radiation exposure dose rate, temperature, dynamics.

1. Introduction

During the active stage of the accident at Chornobyl NPP Unit 4, as a result of chaotic and uncontrolled processes of interaction of the overheated nuclear fuel of the destroyed reactor with various materials, in the lower part of its shaft, a silicate melt was formed. This melt spread in lava-like masses from the melting epicenter (305/2 rooms) and solidified in various rooms in the form of black, brown, and polychrome fuel-containing materials (FCM) [1, 2]. According to state-of-the-art concepts, FCM nuclearly hazardous clusters (NHC), which can contain from 15 to 20 t of uranium, are located in the south-eastern part of the 305/2 room in the areas of intensive concrete ablation of the sub-reactor slab. The monographs [1, 2] present in detail a wide range of scientific publications devoted to the results of many years of experimental and theoretical work on the assessment of the current and forecast state of the NHC before the construction of the New Safe Confinement (NSC). After the NSC was commissioned, the temperature and humidity regime in the "Shelter" rooms changed. As shown by the results of modelling studies [3, 4], a change in the humidity of NHC, which were, as is believed, in a subcritical state until now, can lead to the beginning of the process of reverse criticality and an increase in the level of their nuclear hazard. Based on known data on the location and geometric parameters of the NHC, the fuel content and its enrichment, etc., an analysis of the possibility of a self-sustaining nuclear chain reaction in a neutron-multiplying environment was conducted in [5]. It is shown that the drying of NHC can lead to the occurrence of a single neutron burst with an amplitude comparable to the amplitude of neutron oscillations in 1990. However, such a burst would have no impact on the environment.

Within the framework of "Shelter" conversion into an environmentally safe system, an Integrated Automated Monitoring System was created [2]. One component of Integrated Automated Monitoring System is the Nuclear Safety Monitoring System (NSMS), which is designed to collect, process, store, and provide operational personnel with the data on neutron flux density (NFD) – covering the energy range from thermal to 1 MeV – and the gamma-radiation exposure dose rate (GDR) – with the energy range from 0.1 to 4 MeV [6]. During the NSMS operation, efforts have been made to analyze accumulated measurement data for early detection of negative trends that may reduce the level of "Shelter" nuclear safety [3, 4]. After critical analysis of the obtained NSMS data [6], the specialized software was developed, deployed, and tested on the computing equipment at the Institute for Safety Problems of Nuclear Power Plants of NAS of Ukraine [7].

The research [8] made it possible to define and compare the general trends in GDR and NFD

dynamics in the “Shelter” rooms after the NSC commission. Two main types of GDR and NFD dynamics were established. The first type is characterized by an increase in NFD alongside and gradual decrease in GDR, while the second type presents a similar change pattern for GDR and NFD, showing a simultaneous reduction in their average annual values.

For all NSMS monitoring points, a gradual decrease of GDR is observed in the “Shelter” rooms. At the same time, for six monitoring points located in the rooms 305/2, it has been established that the greater the mean annual rate of NFD growth, the slower GDR declines as compared to the decay rate of radionuclide ^{137}Cs [8]. The established phenomena must be re-examined using the most recent NSMS data and results of concrete temperature and air humidity monitoring around the NHC localization area.

This paper aims to verify previously observed phenomena in the NFD and GDR dynamics features, taking into account the monitoring data for concrete temperature in the 305/2 “Shelter” room and relative humidity (RH) in rooms around the NHC localization area.

2. Objective of this work, measuring equipment, and methods of data analysis

The objective of this work was to analyze the data obtained from the NSMS [6–8] (NFD and GDR) as well as the results of temperature measurements of concrete obtained from the Expert Research System described in [9]. In addition, RH data were collected in two “Shelter” rooms using DLT-11-Pt loggers [10] and Elitech RC-4HC type recorders [11].

At this research stage, NFD, GDR, and concrete temperature data were analyzed for the period of 2017–2024. The layout of NFD and GDR sensor assemblies (SA) and temperature sensors (TS) is shown in Fig. 1. Location details of SA and TS monitoring points in the local coordinate system of ChNPP Unit 4 are listed in [8, 9]. The layout of all sensors is presented as a projection onto the plane of +9.10 m elevation, which corresponds to the top of the NHC model adopted in [3]. The RH loggers were installed in rooms closest to 305/2, based on the possibility of their maintenance and taking readings to a flash drive in existing gamma-radiation fields. Specifically, they were placed in rooms 318/2 at +9.00 m on the table near the wellhead B-12-76 in building axes 44-46 and Ж-И; rooms 207/4 at +6.00 m, in axes Ж-И, 48-49.

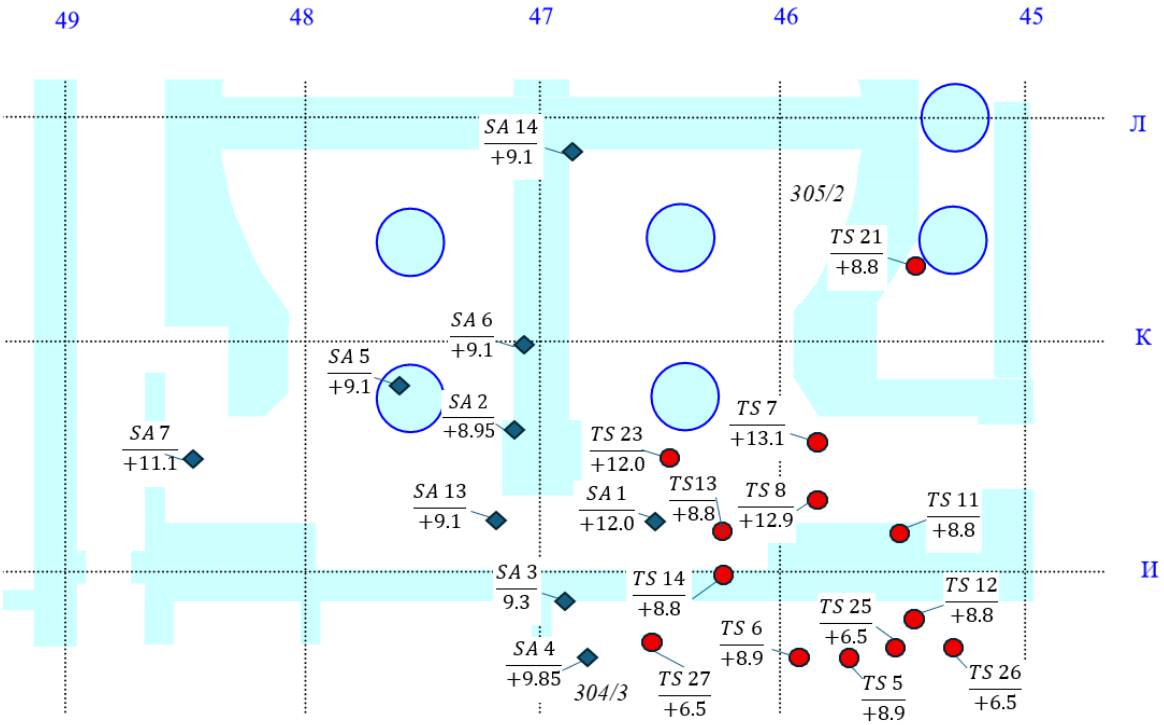

Fig. 1. The layout of NFD and GDR SA and concrete TS onto the plane of +9.10 m elevation in the 305/2 room. (See color Figure on the journal website.)

Mathematical processing of NFD and GDR measurement data and calculation of regression equations parameters were performed using specialized application software [7]. Following the approach in [8], to assess the identified NFD and GDR trends in each monitoring point and compare them, the values

of relative annual average rate of change for GDR (V_g) or NFD (V_n) were calculated:

$$V_{g(n)} = \frac{1}{6} \cdot \sum_{i=2018}^{2023} \left(\frac{N_{i+1} - N_i}{N_i} \right) \cdot 100\ \%,$$

where N_i and N_{i+1} represent annual average values of GDR or NFD for the previous and following year, respectively.

The calculated values of V_g and V_n were checked for the presence of correlation between them and with the annual average values of NFD. The V_g values were compared to the decay rate of ^{137}Cs radionuclide (V_{Cs} = –2.28 % per yr), based on its half-life of 30.1 yr.

To visually illustrate the effect of slowing GDR decline (V_g significantly lower than V_{Cs} value) at the monitoring points where the most intensive growth of V_n value was observed, the parameter A_v, as the absolute difference between V_{Cs} and V_g ($A_v = V_{Cs} - V_g$), was calculated in [8]. Later, the calculation results were checked for the presence of correlation not only between A_v and V_n, but also between A_v, V_n, and NFD annual average values.

In addition, for monitoring points located around the NHC localization area, a study was conducted to identify the correlation between the daily average values of GDR and NFD, on the one hand, and the concrete temperature and RH, on the other hand. Unfortunately, due to the occupation of the Chornobyl Exclusion Zone by russian forces, all computer servers and workstations were looted or destroyed, and RH data in the period 2017–2022 were lost. RH monitoring was fully restored in autumn 2023 after installation and adjustment of new equipment. The presence of a small number of RH observations for rooms 318/2 and 207/4 (2023–2024) limited the time frame for which a correlation analysis was carried out.

3. Results and discussion

Computer data processing using the developed software made it possible to investigate the dynamics of GDR and NFD values from 2018 to 2024 (Table 1), to assess the features of these trends, and to determine the regression equations (Table 2). The data presented below show the results of analysis for NFD and GDR monitoring points located exclusively in room 305/2 (see Fig. 1). Based on analysis of obtained data, it was established that the GDR and NFD dynamics correspond to a single type, an example of which is illustrated in Fig. 2. This type is characterized by the opposing linear trends in the behaviour of monitored parameters: while the NFD gradually increases, the GDR drops (see Table 2).

Table 1. **Average annual GDR (R·h^{-1}) and NFD (n·cm^{-2}·s^{-1}) values in 305/2 rooms**

SA	Monitoring parameter	Monitoring period, yr						
		2018	2019	2020	2021	2022	2023	2024
01	GDR	318.7 ± 1.5	313.4 ± 1.6	307.8 ±1.7	302.2 ± 1.8	296.7 ± 1.6	290.9 ± 2.1	285.1 ± 1.7
	NFD	524.7 ± 19.2	534.7 ± 20.1	539.7 ± 19.7	542.7 ± 19.5	548.4 ± 18.1	550.4 ± 17.1	551.4 ± 20.9
02	GDR	51.5 ± 0.2	50.7 ± 0.3	49.7 ± 0.3	48.8 ± 0.3	47.7 ± 0.3	46.7 ± 0.3	45.7 ± 0.3
	NFD	12.1 ± 0.6	12.8 ± 0.6	13.3 ± 0.6	13.9 ± 0.6	14.2 ± 0.9	12.9 ± 0.6	13.3 ± 0.6
03	GDR	25.4 ± 0.1	25.3 ± 0.2	24.6 ± 0.1	24.2 ± 0.2	23.7 ± 0.2	23.1 ± 0.1	22.6 ± 0.1
	NFD	63.6 ± 2.8	68.2 ± 2.9	73.5 ± 3.1	78.7 ± 3.0	83.0 ± 3.4	89.3 ± 4.1	94.7 ± 3.8
05	GDR	403.4 ± 2.8	399.8 ± 2.6	386.8 ± 5.6	386.0 ± 0.3	384.9 ± 0.6	379.5 ± 2.0	373.4 ± 1.8
	NFD	1516 ± 208	1976 ± 264	2629 ± 1655	2735 ± 114	2647 ± 191	2572 ± 123	2536 ± 151
06	GDR	13.0 ± 0.1	13.0 ± 0.1	12.8 ± 0.1	12.5 ± 0.1	12.2 ± 0.1	11.9 ± 0.1	11.6 ± 0.1
	NFD	28.3 ± 1.0	29.0 ± 1.1	32.9 ± 1.4	36.6 ± 1.4	39.4 ± 1.4	40.7 ± 1.2	41.7 ± 1.3
07	GDR	1.01 ± 0.02	1.01 ± 0.01	0.99 ± 0.01	0.97 ± 0.01	0.96 ± 0.01	0.93 ± 0.01	0.91 ± 0.01
	NFD	95.3 ± 6.6	107.9 ± 5.5	118.6 ± 5.8	129.7 ± 6.2	136.4 ± 5.3	142.4 ± 4.9	138.7 ± 5.5
13	GDR	2.21 ± 0.03	2.19 ± 0.01	2.13 ± 0.02	2.09 ± 0.02	2.04 ± 0.02	1.99 ± 0.02	1.94 ± 0.04
	NFD	6.16 ± 0.91	7.11 ± 0.75	7.25 ± 0.48	7.20 ± 0.48	7.19 ± 0.48	6.98 ± 0.46	7.0 ± 0.40
14	GDR	22.5 ± 0.2	21.9 ± 0.2	21.3 ± 0.2	20.7 ± 0.2	20.2 ± 0.2	19.5 ± 0.2	18.9 ± 0.2
	NFD	116.9 ± 6.1	125.4 ± 6.3	133.8 ± 6.5	141.9 ± 5.7	147.4 ± 5.0	153.4 ± 6.1	155.3 ± 6.2

Note. Values are given as mean ± standard deviation, GDR in R·h^{-1}; NFD in n·cm^{-2}·s^{-1}.

Table 2. **Results of regression analysis of NFD and GDR average daily values, and assessment of relative annual average rate of change (drop or increase) for GDR (V_g) and NFD (V_n)**

SA	Monitoring parameter	Regression equation and coefficient of determination		Difference between prognosis and measurement results, %	V_g or V_n values, %/yr	
		Y = A·x + B	R^2		2018–2022 [8]	2018–2024
01	GDR	–0.016 x + 316.7	0.99	+1.8	–1.7	–1.8
	NFD	0.008 x + 534.6	0.24	+2.2	1.1	**0.8**

Continuation of Table 2

SA	Monitoring parameter	Regression equation and coefficient of determination		Difference between prognosis and measurement results, %	V_g or V_n values, %/yr	
		Y = A·x + B	R^2		2018–2022 [8]	2018–2024
02	GDR	–0.003 x + 51.3	0.99	+1.4	–1.8	–2.0
	NFD	0.00013 x+13.2	0.02	–1.2	4.7	3.9
03	GDR	–0.0014 x +25.4	0.98	+2.4	–1.7	–1.9
	NFD	0.014 x + 66	0.98	–7.7	7.6	6.9
05	GDR	–0.013 x + 399.5	0.87	+1.5	–1.1	–1.3
	NFD	0.031 x + 2588	0.001	+5.0	18.8	10.0
06	GDR	–0.0008 x + 13.2	0.98	+3.0	–1.5	–1.9
	NFD	0.007 x + 29.2	0.92	+1.6	9.9	6.8
07	GDR	–0.00005 x + 1	0.99	+1.0	–1.3	–1.7
	NFD	0.018 x + 109.7	0.82	+0.7	11.0	6.6
13	GDR	–0.0001 x + 2.2	0.96	+3.3	–1.9	–2.1
	NFD	0.00005 x + 7.2	0.15	–1.5	4.3	2.3
14	GDR	–0.0016 x + 22.2	0.99	+3.1	–2.5	–**2.9**
	NFD	0.017 x + 124.8	0.92	+1.2	6.2	4.9

Note. Y for GDR – in $R \cdot h^{-1}$, for NFD – in $n \cdot cm^{-2} \cdot s^{-1}$, X – full day from 01.01.2018 to 31.12.2024.

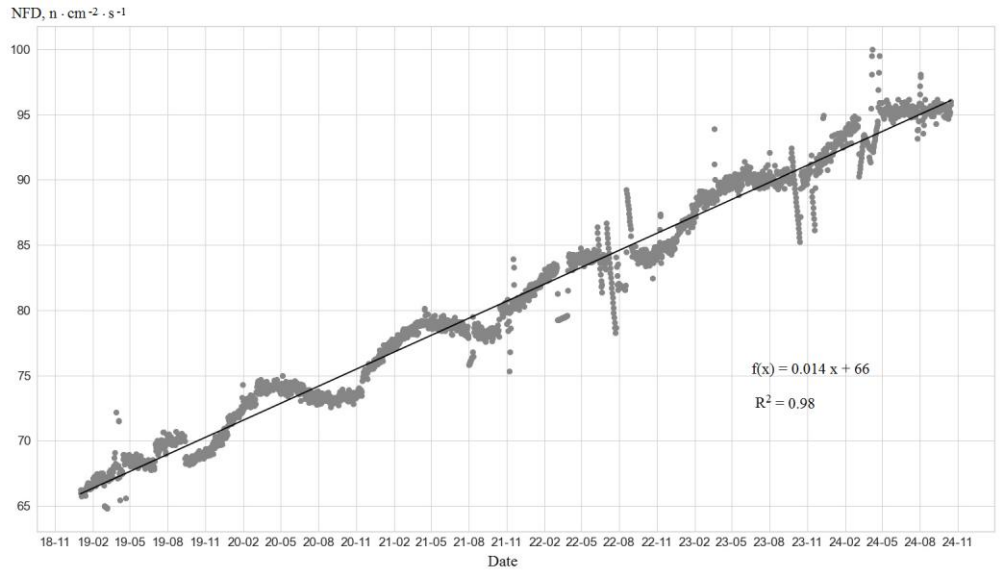

a

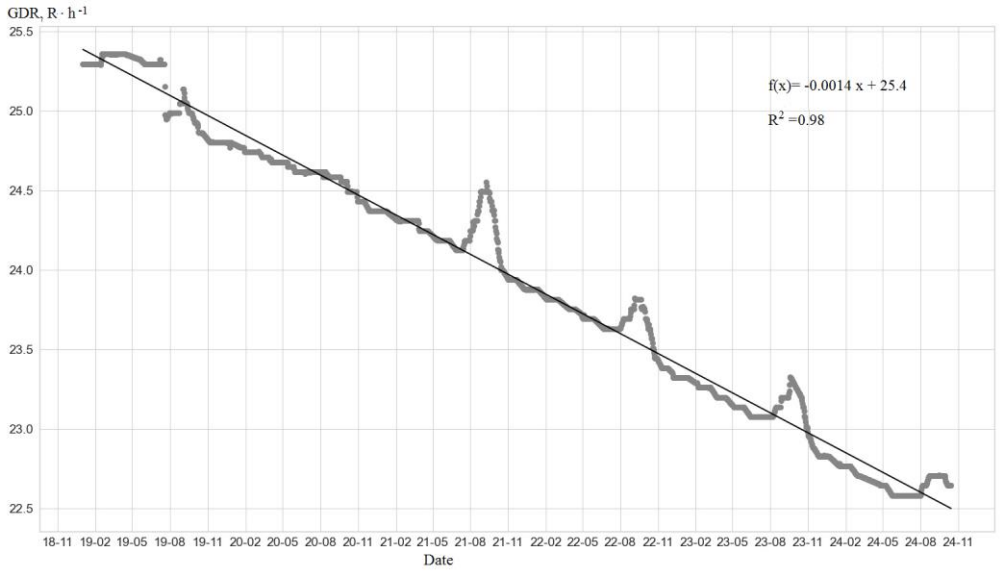

b

Fig. 2. Example of opposite linear trends in NFD (*a*) and GDR (*b*) dynamics in "Shelter" room 305/2. Types of trends, parameters of the linear regression equation, and the coefficient of determination are given for SA 03.

In the dynamics of NFD and GDR average daily values, there may be occasional anomalous results that significantly differ in amplitude, both higher and lower, compared to the predominant number of other results corresponding to the above-mentioned tendency (trend). The most noticeable anomalous results were present in the NFD dynamics registered by SAs 02, 05, and 13. As a result, these anomalies affected the value of determination coefficient (R^2) for regression equation presented in Table 2, and Pearson's linear correlation coefficient (r, $r^2 = R^2$) between daily annual GDR and NFD values in different SAs (Fig. 3). The designations NFD001- NFD016 and GDR001- GDR016 in Fig. 3 correspond to the abbreviated names of NFD and GDR sensors as part of the relevant SAs presented in Tables 1 and 2.

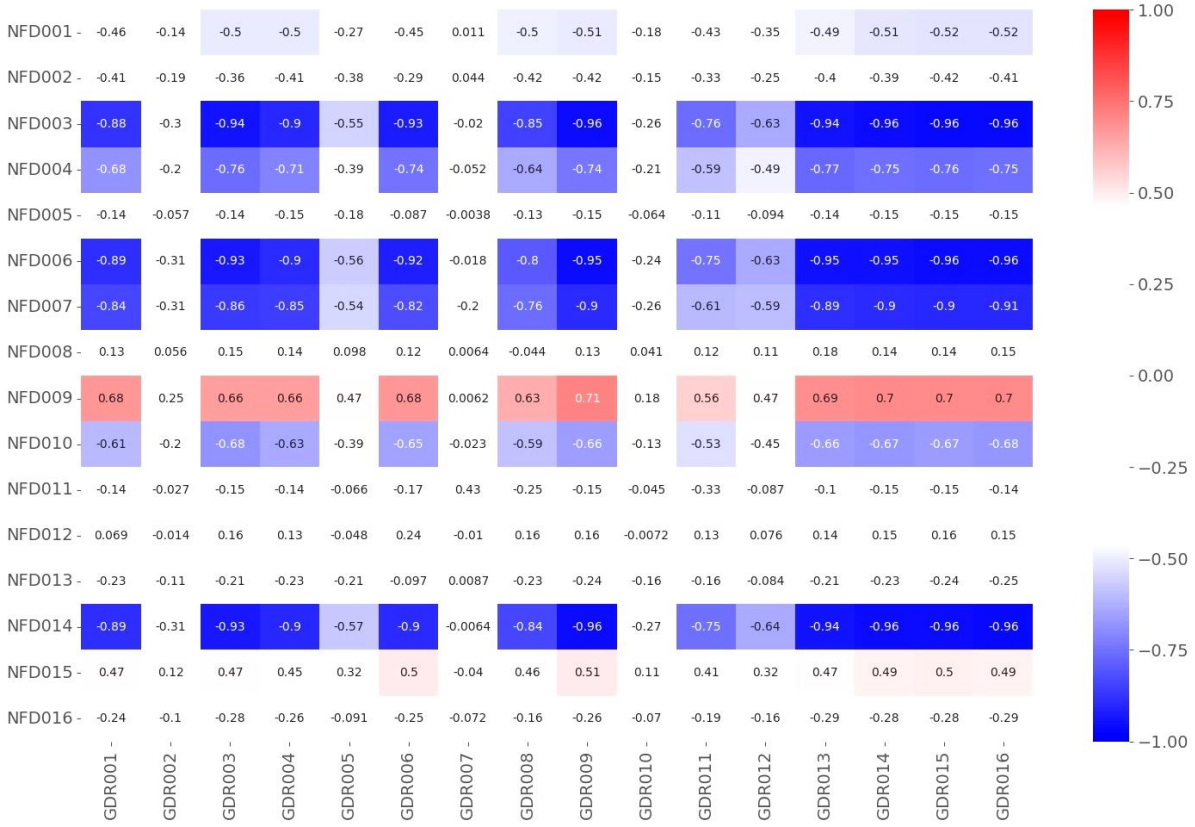

Fig. 3. Pearson's linear correlation coefficients between average daily GDR and NFD values in different SAs (2018–2024). (See color Figure on the journal website.)

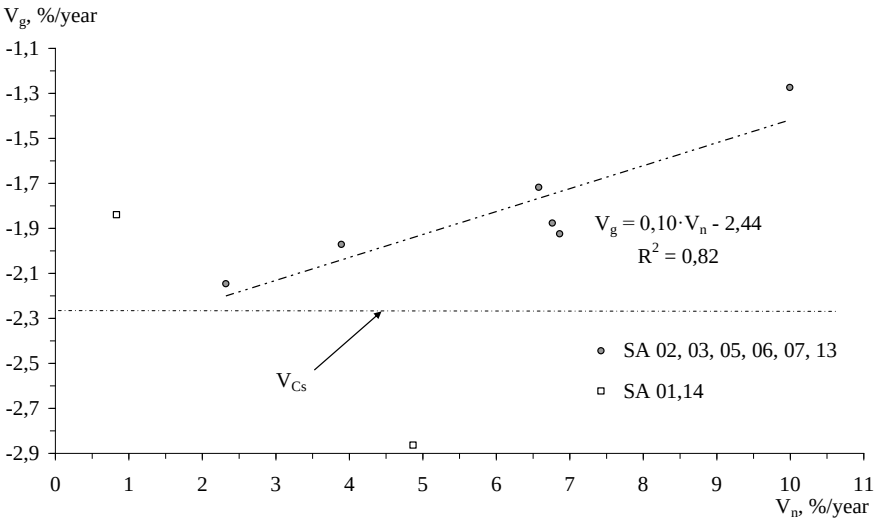

Fig. 4. Linear functional dependence between GDR (V_g) and NFD (V_n) change rates in "Shelter" room 305/2 against the background of decay rate of ^{137}Cs (V_{Cs}). For SA 01 and SA 14 data represent two opposite cases that were not typical of the general trend observed.

The data presented in Table 2 and Fig. 3 confirm the presence of a weak to strong negative linear correlation between the average daily NFD and GDR values near the NHC FCM localization area in room 305/2. As shown in Table 2, regression equations describe detected trends in the change of average daily values of the control parameters with considerable accuracy. The difference between the predicted and measured (01/01/2025) values did not exceed 3.3 % for GDR and 7.7 % for NFD, including data for SA 02, 05, and 13.

Fig. 4 presents the data from Table 3 in graphical form, confirming the findings in [8] regarding the existence of a close relationship between the relative annual average rate of change for GDR (V_g) and NFD (V_n). As illustrated in Fig. 4, the higher V_n value corresponds to a larger deviation of the V_g value (toward lower values) from the decay rate of the main dose-forming radionuclide ^{137}Cs.

Table 3. **Average annual concrete temperature around the area of FCM NHC localization, °C**

No. group	Item of TS and "Shelter" rooms	Monitoring period, yr							
		2017	2018	2019	2020	2021	2022	2023	2024
1	TS 7 (305/2)	17.8 ± 1.5	19.5 ± 3.2	23.1 ± 1.1	23.8 ± 0.9	23.3 ± 1.9	22.7 ± 1.4	21.9 ± 2.7	22.5 ± 2.6
	TS 8 (305/2)	16.6 ± 1.4	18.4 ± 3.1	21.5 ± 1.1	22.2 ± 0.7	22.9 ± 1.8	22.4 ± 0.3	22.2 ± 2.2	22.6 ± 2.1
	TS 23 (305/2)	13.0 ± 2.4	14.4 ± 4.9	18.7 ± 1.8	19.3 ± 1.7	18.2 ± 2.0	17.6 ± 0.6	17.5 ± 2.3	17.8 ± 2.2
2	TS 5 (304/3)	15.2 ± 1.7	16.9 ± 3.2	20.7 ± 1.2	21.6 ± 1.1	21.7 ± 0.9	21.2 ± 0.4	21.3 ± 0.9	21.4 ± 1.0
	TS 6 (304/3)	14.6 ± 1.3	16.0 ± 3.2	19.7 ± 1.0	20.7 ± 1.0	22.0 ± 1.0	21.4 ± 0.5	21.4 ± 1.7	21.7 ± 1.5
	TS 11 (305/2)	15.2 ± 1.7	16.9 ± 3.2	20.7 ± 1.2	21.5 ± 1.0	21.1 ± 1.0	20.3 ± 0.4	20.4 ± 1.0	20.8 ± 1.1
	TS 12 (304/3)	14.6 ± 1.3	16.0 ± 3.2	19.7 ± 1.0	20.6 ± 1.0	20.1 ± 1.0	19.4 ± 0.4	19.4 ± 1.0	19.7 ± 1.1
	TS 13 (305/2)	17.8 ± 1.5	19.5 ± 3.2	23.1 ± 1.1	23.9 ± 0.9	23.3 ± 1.1	22.8 ± 0.4	22.7 ± 1.0	23.0 ± 1.1
	TS 14 (304/3)	16.6 ± 1.4	18.4 ± 3.1	21.5 ± 1.1	22.2 ± 0.7	21.9 ± 1.1	21.3 ± 0.3	21.3 ± 1.0	21.5 ± 1.1
	TS 21 (307/2)	18.8 ± 2.6	18.2 ± 3.1	21.9 ± 0.9	22.7 ± 0.9	22.2 ± 1.0	21.6 ± 0.4	21.6 ± 1.0	21.8 ± 1.0
	TS 25 (210/5)	15.1 ± 2.7	15.9 ± 3.1	19.0 ± 0.9	19.9 ± 0.8	19.2 ± 0.9	18.6 ± 0.2	18.6 ± 0.9	18.9 ± 1.0
	TS 26 (210/5)	14.9 ± 2.6	15.8 ± 3.1	18.9 ± 0.9	19.4 ± 0.6	19.0 ± 0.8	18.5 ± 0.2	18.4 ± 0.8	18.7 ± 0.9
	TS 27 (210/6)	15.6 ± 2.3	16.3 ± 3.2	19.0 ± 0.9	19.8 ± 0.9	19.2 ± 0.8	18.6 ± 0.2	18.6 ± 0.8	18.9 ± 0.9

Note. Values are given as mean ± standard deviation.

The linear trend derived from a wider data sample was found to be more moderate as compared to previously known data [8] (Table 4). However, the present results provide clearer evidence that this phenomenon indeed exists, and it is a characteristic feature of NFD and GDR dynamics at the monitoring points located in room 305/2 only.

Table 4. **Regression equations parameters of average monthly values of concrete temperature**

No. group	Item of TS and "Shelter" rooms	Parameter of the regression equation Y = A·x + B						Difference between T_p and T_m, %
		A_1	B_1	R_1^2	A_2	B_2	R_2^2	
1	TS 7 (305/2)	0.0064	–257.6	0.67	–0.00003	21.4	0,02	+0.2
	TS 8 (305/2)	0.0042	–161.0	0.66	0.0015	16.0	0,01	–21.0
	TS 23 (305/2)	0.0076	–312.7	0.53	–0.0004	18.0	0,01	–4.6
2	TS 5 (304/3)	0.0050	–197.3	0.65	0.00005	19.1	0,01	–4.5
	TS 6 (304/3)	0.0055	–222.3	0.74	0.001	22.1	0,002	+2.9
	TS 11 (305/2)	0.0068	–277.1	0.70	–0.0002	28.5	0,04	+28.8
	TS 12 (304/3)	0.0065	–264.5	0.68	–0.0002	26.7	0,10	+27.6
	TS 13 (305/2)	0.0065	–262.8	0.70	–0.0002	30.2	0,10	+24.1
	TS 14 (304/3)	0.0060	–239.0	0.66	–0.0001	28.2	0,04	+25.2
	TS 21 (307/2)	0.0052	–206.7	0.52	–0.0002	20.2	0,10	–12.0
	TS 25 (210/5)	0.0056	–226.0	0.60	–0.0002	25.8	0,10	+28.8
	TS 26 (210/5)	0.0053	–211.4	0.56	–0.0002	25.2	0,10	+27.7
	TS 27 (210/6)	0.0050	–200.0	0.55	–0.0008	33.1	0,23	–

Note. The subscripts 1 and 2 in the parameters of regression correspond to the first and second monitoring periods, respectively. The unit of measurement x in the regression equation is days; the number of days is calculated from the beginning of the corresponding monitoring period.

According to the available data, a different pattern is observed: there is a tendency for the V_g (A_v) and V_n values to increase with increasing NFD, and the shape of this dependence is close to logarithmic with $R^2 = 0.78$ for V_g (A_v) and $R^2 = 0.81$ for V_n. However, the lack of data on V_g (A_v) and V_n in the range of NFD values from 500 to 2500 $n \cdot cm^{-2} \cdot s^{-1}$ requires further clarification of the parameters of the established pattern.

The data presented in Tables 3 and 4 show the results of the analysis of concrete temperature data. As shown in Table 3, the dynamics of concrete temperature around the NHC localization area revealed two monitoring periods: 1 – a period of sustainable increase in the average annual concrete temperature – 2017 - 2020; 2 – a period of relative stabilization of average annual concrete temperature against the background of seasonal fluctuation in average monthly temperature – 2021–2024. Despite the relatively low R^2 values, the regression equations for the second period describe the observed trends in the change of average monthly concrete temperature quite accurately. The difference between the predicted (T_p) and measured (T_m) concrete temperature values on 10/01/2025 (see Table 4) did not exceed 30 %, the average difference is equal to 0.4 %. Comparison for TS 27 was not carried out due to the failure of the temperature sensor (August 2024). It was determined that TS can be split into two groups (see Tables 3 and 4), which differ, firstly, in distance from the area NHC localization (see Fig. 1), and secondly, in features in the dynamic of the average monthly temperature (time when it's maximum and minimum values). Examples of typical concrete temperature dynamics among the groups are shown in Figs. 5 and 6, *a*.

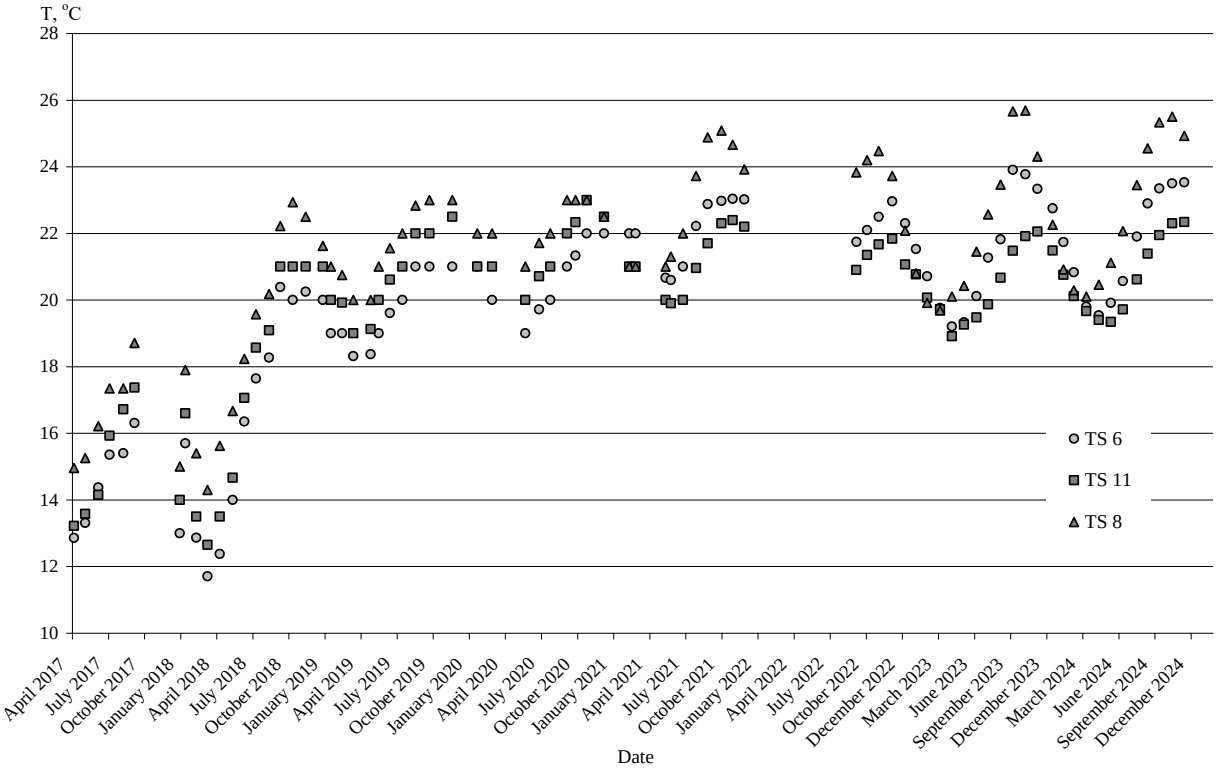

Fig. 5. Typical form of dynamics of average monthly concrete temperature around the area of NHC FCM localization. Examples for TS belong to group 1 (TS 8) and group 2 (TS 6, TS 11).

Fig. 6 illustrates how significantly the seasonal fluctuations of average monthly values (time when it's maximum and minimum values) differ between concrete temperature (Fig. 6, *a*) and air RH in the rooms 207/4 and 318/2 (Fig. 6, *b*). The correlation between the average monthly RH values in these rooms is estimated as strong (r = 0.91). The correlation between the concrete temperature at monitoring points in group 1 (see Table 3) and RH is estimated from very weak to weak (r = 0.11–0.29), then for group 2 it is generally from weak to medium (r = 0.21–0.68). The evident correlation was found between the concrete temperature at the monitoring points in group 2 and the RH in room 318/2 (r = 0.54–0.68), which gives grounds to assume that their seasonal fluctuations are generally synchronous.

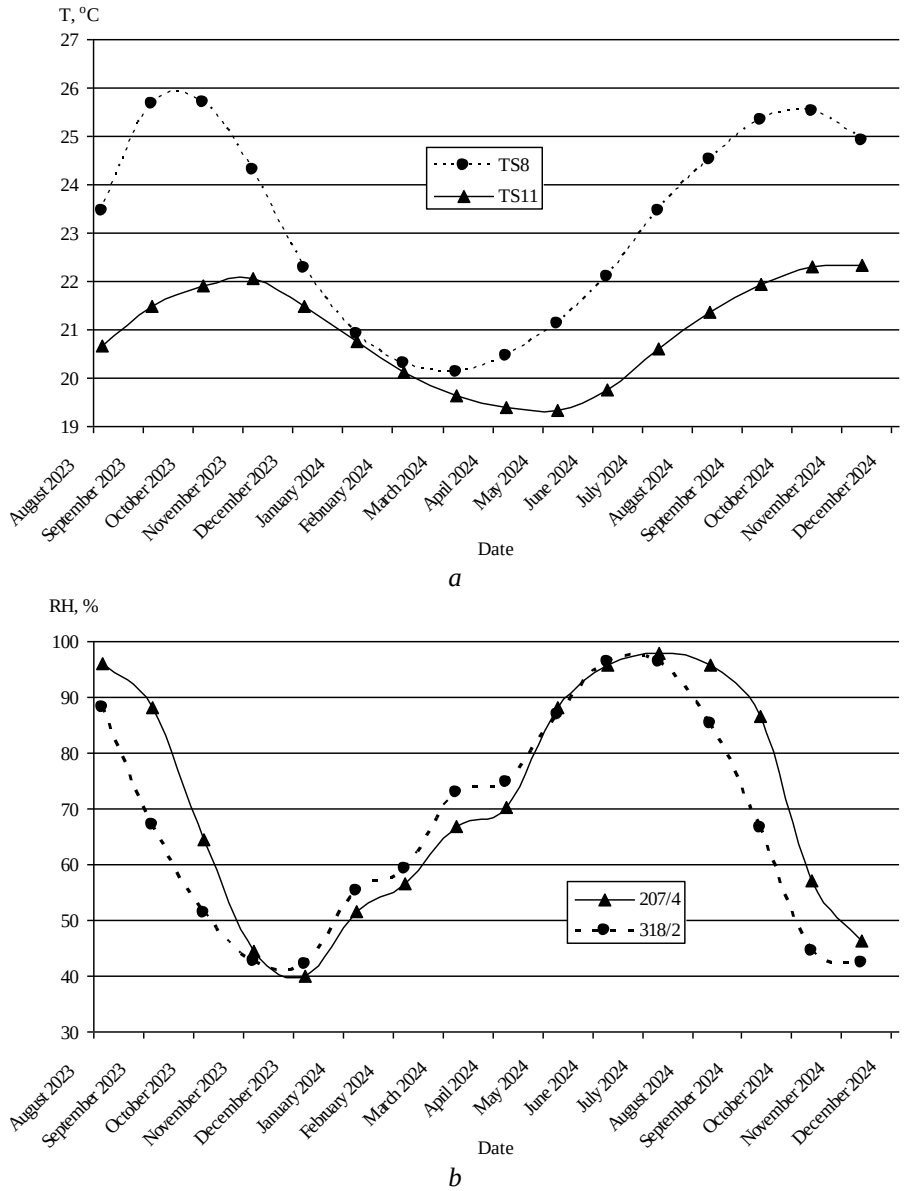

Fig. 6. Seasonal variations in concrete temperature (*a*) and air humidity (*b*) in "Shelter" rooms.

Prior to NSC installation in its design position, the temperature gradients in concrete around the NHC localization area in the "Shelter" room 305/2 were estimated with the following values: for the eastern direction – 0.65–1.34 ºC/m; for the western and south-western directions – 0.60–1.68 ºC/m; for the south-eastern and southern directions – 0.42–1.54 ºC/m [7]. It was indicated that the temperature gradients in concrete are now in the following ranges: for the eastern direction – 0.48–0.58 °C/m; for the south-eastern and southern directions – 0.42–1.02 °C/m. Unfortunately, for western and south-western directions, such assessments remained unavailable due to the lack of opportunity to increase the network of monitoring points. Thus, after the NSC installation in the design position, the temperature gradients in the concrete have decreased, but still provide the necessary conditions for heat dissipation from the FCM NHC surface. Furthermore, the previously observed growth in average annual concrete temperature ceased in 2020–2021.

To search for correlations between the NFD or GDR, on the one hand, and the concrete temperature, on the other hand, NFD sensors were selected, the data for which were previously analyzed in the works devoted to the assessment of the subcriticality level of FCM clusters in the "Shelter" [3, 4]. The following conclusions were made based on the correlation analysis results. The correlation between NFD or GDR and concrete temperature is very weak or moderate for average monthly values: for NFD – concrete temperature r = 0.12–0.37, for GDR – concrete temperature r = 0.10–0.48.

In work [4], it was first noted that NFD seasonal fluctuations may be caused by RH periodic changes in the "Shelter" rooms (the appearance of condensation). According to correlation analysis results, it

was found that the correlation between NFD and RH varies from very weak to medium (r = 0.01–0.69). Similarly, the correlation between GDR and RH ranged from very weak to strong (r = 0.06–0.71). A significant difference in the correlation between NFD and RH at rooms 207/4 and 318/2 was observed only for SA 03 (r is equal to 0.01 and 0.40, respectively). For GDR, no such substantial difference was found. The highest correlation between NFD and RH in 207/4 rooms was determined for SA's 04, 07 and 13 (r = 0.55–0.69), between NFD and RH in 318/2 rooms – for the locations of SA's 03, 04, 07 and 13 (r = 0.40–0.55), between GDR and air humidity – only for SA 13 (r is equal to 0.61 and 0.71 for rooms 207/4 and 318/2, respectively).

Thus, the hypothesis stated in [4] about the relationship between NFD and RH in "Shelter" – that the NFD growth is restrained during the condensation period and increases during the evaporation period – is only partially confirmed by the observations in 2023–2024. For SA's 01 and 06, the correlation between NFD and RH is very weak (r < 0.1), indicate ng that it is, practically, absent. However, if we refer to the data in Table 1, it can be assumed that the moderate and medium correlations with RH are typical for low and medium levels of NFD.

4. Conclusions

The research enabled the clarification and comparison of the general trends in GDR and NFD dynamics around the area of FCM with high uranium content in the "Shelter" rooms 305/2 after the NSC commission for the period 2017–2024. Only one type of average monthly NFD and GDR dynamics was identified: an increase in NFD alongside a gradual decrease in GDR, observed against the background of seasonal fluctuations. The data suggest that the greater the mean annual rate of NFD growth, the more slowly GDR declines as compared to the decay rate of the main dose-forming radionuclide ^{137}Cs.

The data have confirmed that, starting from 2020–2021, the period of growth of the average annual concrete temperature, which was observed after the NSC arch was installed in the design position, was replaced by a period of its relative stabilization against the background of seasonal fluctuations in the average monthly values of concrete temperature and air humidity in the "Shelter" rooms. Correlation analysis results showed that seasonal fluctuations in concrete temperature and air humidity are, generally, synchronous.

Results of the study showed that:

– Between NFD or GDR and concrete temperature for average monthly values in locations closest to NHC area localization, correlations range from very weak to medium.

– There is a possibility that moderate and medium correlations between NFD and air humidity are typical for low and medium levels of NFD only.

Given the NHC potential danger and the data on the NFD and GDR features, it is necessary to continue monitoring the state of such FCM. Clarification of the physical nature of the established relationships and correlations is impossible without the use of advanced mathematical analysis tools - such as time series analysis methods, Monte Carlo methods, etc. The research results presented can be used not only to refine the models of NHC behaviour and predict the levels of their criticality. This opens up prospects for a deeper understanding of the phenomena recorded at the empirical level and the identification of hidden patterns, which is very important for ensuring the "Shelter" safety in the future.

The participation in writing this article provided by Valentyn Bezmylov, Leading Engineer of ISP NPP NAS of Ukraine, is gratefully acknowledged by the authors.

REFERENCES

1. V. O. Krasnov et al. *Object "Shelter": 30 Years After the Accident*. Monograph (Chornobyl: Institute for Safety Problems of Nuclear Power Plants, NAS of Ukraine, 2016) 512 p. (Ukr)
2. V.O. Krasnov et al. *The Shelter Object in Conditions of the New Safe Confinement.* A.V. Nosovskyi (Ed.) (Chornobyl: Institute for Safety Problems of Nuclear Power Plants, NAS of Ukraine, 2021) 344 p. (Ukr)
3. E.D. Vysotsky, R.L. Godun, A.O. Doroshenko. The dynamics of neutron activity and subcriticality of a nuclear-dangerous cluster in the conditions of NSC-SO complex. Problems of Nuclear Power Plants' Safety and of Chornobyl 30 (2018) 78. (Rus)
4. Ye.D. Vysotskyi, K.O. Sushchenko, R.L. Godun. Expert assessment of the current criticality level of clusters of fuel-containing materials after the New Safe Confinement installing. Nuclear Power and the Environment 16 (2020) 49. (Rus)
5. V.M. Pavlovych, V.A. Babenko. On the possibility of the self-sustaining nuclear chain reaction inside the "Shelter" object at the present time. Nucl. Phys. At. Energy 24 (2023) 239. (Ukr)
6. M.V. Saveliev et al. The nuclear safety monitoring system for fuel-containing materials located in destroyed Unit No. 4 of the Chornobyl NPP and proposals for its modernization. Nucl. Phys. At. Energy 23 (2022) 172.
7. M.V. Saveliev, O.V. Mykhailov, D.O. Sushchenko.

Analysis of exposure dose rate and neutron flux density dynamics in the Shelter object of the Chornobyl NPP. Nuclear Power and the Environment 25 (2022) 24. (Ukr)
8. O.V. Mykhailov et al. Features of neutron flux density and gamma-radiation exposure dose rate dynamics in ChNPP Shelter Object after the New Safe Confinement commissioning. Nuclear Power and the Environment 27 (2023) 44.
9. O.V. Mykhailov, A.O. Doroshenko, M.V. Saveliev. Results of analysis of temperature monitoring data around the nuclearly hazardous cluster of fuel-containing materials in the sub-reactor room 305/2 of the "Shelter" object, inside and outside the new safe confinement. Nucl. Phys. At. Energy 25 (2024) 349.
10. DLT-10 / DLT-11 Manual. Temperature and Humidity Loggers (Portable Recorders) [Electronic resource] (Kharkiv: AO TERA LLC, [n. d.]) 14 p.
11. Elitech Technology, Inc. Quick Start Guide RC-4 / RC-4HA / RC-4HC. Temperature and Humidity Data Loggers [Electronic resource] (Elitech Technology, Inc., [n. d.]) 8 p.

О. В. Михайлов*, М. В. Савельєв, А. О. Дорошенко

Інститут проблем безпеки АЕС НАН України, Чорнобиль, Україна

*Відповідальний автор: o.mikhailov@ispnpp.kiev.ua

АНАЛІЗ ДАНИХ БАГАТОРІЧНОГО МОНІТОРИНГУ НАВКОЛО ЗОНИ ЛОКАЛІЗАЦІЇ ЯДЕРНО-НЕБЕЗПЕЧНИХ СКУПЧЕНЬ В ОБ'ЄКТІ «УКРИТТЯ»

Представлено результати комплексного аналізу даних щодо щільності потоку нейтронів (ЩПН), потужності експозиційної дози (ПЕД) гамма-випромінювання та температури бетону поблизу ядерно-небезпечних скупчень паливовмісних матеріалів (ЯНС ПВМ) у приміщенні 305/2 Чорнобильського об'єкта «Укриття». За даними системи контролю ядерної безпеки встановлено характерні тенденції динаміки ЩПН та ПЕД за період з 2017 до 2024 року. Досліджено сезонні коливання вологості повітря, температури бетону та їхній вплив на динаміку ЩПН. Визначено, що кореляційний зв'язок між виміряними параметрами, від слабкого до щільного, залежить від місця розташування датчика відносно зони локалізації ядерно-небезпечного скупчення паливовмісних матеріалів у бетоні підреакторної плити. Отримані дані підтверджують важливість постійного моніторингу з метою забезпечення ядерної безпеки об'єкта «Укриття» та продовження досліджень у цьому напрямку.

Ключові слова: Чорнобильська АЕС, об'єкт «Укриття», ядерно-небезпечні скупчення, щільність потоку нейтронів, потужність експозиційної дози, температура, динаміка.

Надійшла / Received 19.06.2025